

See discussions, stats, and author profiles for this publication at: <http://www.researchgate.net/publication/236657692>

# Cotransport of *Pseudomonas putida* and kaolinite particles through water-saturated columns packed with glass beads

ARTICLE *in* WATER RESOURCES RESEARCH · FEBRUARY 2011

Impact Factor: 3.71 · DOI: 10.1029/2010WR009560

---

CITATIONS

21

DOWNLOADS

46

VIEWS

70

## 2 AUTHORS:



[Ioanna A. Vasiliadou](#)

King Juan Carlos University

22 PUBLICATIONS 221 CITATIONS

[SEE PROFILE](#)



[Constantinos V. Chrysikopoulos](#)

Technical University of Crete

143 PUBLICATIONS 1,991 CITATIONS

[SEE PROFILE](#)

## Cotransport of *Pseudomonas putida* and kaolinite particles through water-saturated columns packed with glass beads

Ioanna A. Vasiliadou<sup>1</sup> and Constantinos V. Chrysikopoulos<sup>1</sup>

Received 17 May 2010; revised 4 November 2010; accepted 11 November 2010; published 24 February 2011.

[1] This study is focused on *Pseudomonas putida* bacteria transport in porous media in the presence of suspended kaolinite clay particles. Experiments were performed with bacteria and kaolinite particles separately to determine their individual transport characteristics in water-saturated columns packed with glass beads. The results indicated that the mass recovery of bacteria and clay particles decreased as the pore water velocity decreased. Batch experiments were carried out to investigate the attachment of *Pseudomonas putida* onto kaolinite particles. The attachment process was adequately described by a Langmuir isotherm. Finally, bacteria and kaolinite particles were injected simultaneously into a packed column in order to investigate their cotransport behavior. The experimental data suggested that the presence of clay particles significantly inhibited the transport of bacteria in water-saturated porous media. The observed reduction of *Pseudomonas putida* recovery in the column outflow was attributed to bacteria attachment onto kaolinite particles, which were retained onto the solid matrix of the column. A mathematical model was developed to describe the transport of bacteria in the presence of suspended clay particles in one-dimensional water-saturated porous media. Model simulations were in good agreement with the experimental results.

**Citation:** Vasiliadou, I. A., and C. V. Chrysikopoulos (2011), Cotransport of *Pseudomonas putida* and kaolinite particles through water-saturated columns packed with glass beads, *Water Resour. Res.*, 47, W02543, doi:10.1029/2010WR009560.

### 1. Introduction

[2] Numerous contaminants, including biocolloids (e.g., bacteria and viruses), are frequently present in the subsurface and are not only dissolved or suspended in the aqueous phase but also attached onto other mobile colloid particles (e.g., clays, humic substances, and metal oxides). Experimental as well as theoretical studies suggest that colloid-facilitated contaminant transport in porous media may contribute to contaminant migration over greater distances than contaminant transport in the absence of colloids [Newman *et al.*, 1993; Abdel-Salam and Chrysikopoulos, 1995a, 1995b; Saiers and Hornberger, 1996; Artinger *et al.*, 2002; Mibus *et al.*, 2007]. Consequently, failure to account for colloid-facilitated contaminant transport in porous media may lead to significantly erroneous predictions [Tatalovich *et al.*, 2000; Bekhit and Hassan, 2007].

[3] Bacteria transport in porous media is affected by physical factors, such as water velocity and cell concentration [Tan *et al.*, 1994; Camesano *et al.*, 1999; Hendry *et al.*, 1999; Stevik *et al.*, 2004]; physiological characteristics, such as cell size and motility [Camper *et al.*, 1993; Camesano and Logan, 1998; Becker *et al.*, 2004]; and cell surface properties, such as lipopolysaccharides and hydrophobicity [Gannon *et al.*, 1991; Simoni *et al.*, 1998; Bolster *et al.*, 2009]. The attachment of bacteria onto the solid

matrix is affected by the nature of bacterial and mineral surfaces as well as by the chemistry of the fluid phase [Jewett *et al.*, 1995; Powelson and Mills, 2001; Choi *et al.*, 2007; Kim *et al.*, 2008]. A decrease in ionic strength results in electrical double-layer expansion, and an increase in pH enlarges the negative charge on colloid surfaces. These solution chemistry changes increase the repulsive forces between suspended particles and collector surfaces and, consequently, may enhance the release of deposited particles [Tong *et al.*, 2005; Shiratori *et al.*, 2007].

[4] Colloids generally range in size from 1 nm to 10  $\mu\text{m}$  [Chrysikopoulos and Sim, 1996] and may be introduced or formed in the subsurface, for instance, as a result of well drilling, leaching from the vadose zone, and dissolution of inorganic cementing agents that bind colloid-size materials to solid surfaces [James and Chrysikopoulos, 1999; Compere *et al.*, 2001]. Clay minerals are the finest inorganic components in soils and sediments and possess a very high surface area to volume ratio and great affinity for bacteria [Rong *et al.*, 2010].

[5] Jiang *et al.* [2007] have reported that the attachment of *Pseudomonas (P.) putida* onto kaolinite, goethite, and montmorillonite decreased gradually in the pH range 3–10. Foppen and Schijven [2005] and Kim *et al.* [2008] have shown with column experiments that *Escherichia (E.) coli* attachment onto goethite-coated sand increased with increasing coated sand content. Leon-Morales *et al.* [2004] investigated the transport of laponite in porous media and its effects on biofilm stability and observed that the presence of laponite influences the detachment of *P. aeruginosa* SG81 biofilm from quartz sand.

<sup>1</sup>Environmental Engineering Laboratory, Civil Engineering Department, University of Patras, Patras, Greece.

[6] Colloid-facilitated contaminant transport in porous media has been experimentally and theoretically investigated for radionuclides [Kersting *et al.*, 1999; Artinger *et al.*, 2002; Mibus *et al.*, 2007; Severino *et al.*, 2007; Tien and Jen, 2007], heavy metals [Barton and Karathanasis, 2003], pesticides [Lindqvist and Enfield, 1992; Villholth *et al.*, 2000], and other chemicals [Ouyang *et al.*, 1996; de Jonge *et al.*, 2004; James *et al.*, 2005]. However, the role that colloids play in the transport of biocolloids (viruses and bacteria) in porous media is not fully understood. Very few studies investigate the combined effects of temperature and agitation on bacteriophage MS2 and  $\Phi$ X174 attachment onto kaolinite and bentonite clay particles [Syngouna and Chrysikopoulos, 2010] and show that mineral colloids, depending on the physicochemical conditions, can enhance or hinder the migration of MS2 in columns packed with aquifer material [Walshe *et al.*, 2010]. Furthermore, bacterial transport [Fontes *et al.*, 1991; Jewett *et al.*, 1995; Auset *et al.*, 2005; Dong *et al.*, 2006; Maxwell *et al.*, 2007; Chrysikopoulos *et al.*, 2010] and bacterial-facilitated contaminant transport [Corapcioglu and Kim, 1995; Pang *et al.*, 2005; Pang and Simunek, 2006] have received considerable attention. Although biocolloids are often released into the subsurface either accidentally from septic tanks, broken sewer lines, improperly constructed landfills, and open dumps or intentionally during artificial recharge with treated municipal wastewater [Yates *et al.*, 1985; Anders and Chrysikopoulos, 2005; Masciopinto *et al.*, 2008], their transport in the presence of other mobile colloids is not well understood.

[7] The present study aims to investigate the cotransport of bacteria and clay particles in water-saturated columns packed with glass beads. Batch experiments were conducted to characterize the attachment of *P. putida* onto kaolinite. Flow-through experiments were performed to investigate the interactions between *P. putida* and kaolinite particles during their simultaneous transport in a packed column.

## 2. Materials and Methods

### 2.1. Bacteria and Culture Preparation

[8] The *P. putida* (ATCC17453) cells were initially cultured in 10 mL of nutrient broth (Laury Pepto Bios Broth 35.6 g/L, Biolife) over a period of 20 h and incubated at a 30°C temperature in a 140 rpm orbital shaker until an optical density at 600 nm (OD<sub>600</sub>) of 0.5 absorbance units (AU) was reached. Subsequently, 5 mL of culture were transferred to 250 mL of the same medium and incubated at 30°C for 20 h.

[9] Cells in the late exponential growth phase (OD<sub>600</sub> = 0.9 AU) were harvested (by centrifugation for 10 min at 3000g) and washed three times with distilled deionized water (ddH<sub>2</sub>O). Harvesting at the end of the logarithmic phase minimizes the potential for cell numbers to increase during the transport experiments. After the washing procedure, bacteria were diluted to ddH<sub>2</sub>O to the desired experimental concentration in colony-forming units (CFU) of approximately  $1.35 \times 10^7$  to  $1.26 \times 10^8$  CFU/mL with an optical density at 410 nm of OD<sub>410</sub> = 0.12–0.79 AU (22–150 mg of total cells/L), respectively. The optical density of bacteria in ddH<sub>2</sub>O was analyzed at a wavelength of 410

nm [Rong *et al.*, 2008] by a UV-VIS spectrophotometer (UV-1100, Hitachi), and the concentration of bacterial cells was calibrated using a standard curve of bacterial optical density on the basis of dry weights.

[10] Removing cells from growth media and resuspending them into distilled deionized water may have affected their motility and even altered their swimming speed. However, microscope examination verified that the cells were motile and still capable of growth as determined by plate counts on agar plates [Liu and Papadopoulos, 1995; Camesano and Logan, 1998].

[11] The zeta potential of the bacterial suspension at pH 7 in ddH<sub>2</sub>O, which was measured by a zeta potential analyzer (ZetaSizer, Malvern Instruments Corporation), was estimated to be  $-44.2 \pm 1.6$  mV. The *P. putida* employed in this work was a rod-shaped bacterium with an average length of  $2.4 \pm 0.9$   $\mu$ m and an average diameter of  $0.9 \pm 0.1$   $\mu$ m, as determined from 50 scanning electron microscopy (SEM) images of cells, and equivalent spherical diameter of  $2.2 \pm 0.4$   $\mu$ m, as estimated by a ZetaSizer analyzer (Malvern Instruments).

### 2.2. Minerals

[12] Fifty grams of kaolinite from Washington County, Georgia (Clay Minerals Society), were mixed with 100 mL of ddH<sub>2</sub>O in a 2 L beaker. Hydrogen peroxide (30% solution) was added to the suspension to oxidize organic matter, while the pH was adjusted to 10 with 0.1 M NaOH. The suspension was diluted to 2 L and the <2  $\mu$ m colloid fraction was separated by sedimentation for a time period of 1 h. The size of the colloids was confirmed using a ZetaSizer analyzer. The separated colloid suspension was flocculated by adding a 0.5 M CaCl<sub>2</sub> solution. The colloid particles were washed with ddH<sub>2</sub>O and ethanol and dried at 60°C [Rong *et al.*, 2008].

[13] The zeta potential of the kaolinite suspension at pH 7 in ddH<sub>2</sub>O was estimated to be  $-22.5 \pm 2.1$  mV. The optical density of kaolinite particles was analyzed at a wavelength of 280 nm by a UV-VIS spectrophotometer, and the concentration of kaolinite was calibrated with a standard curve of kaolinite optical density on the basis of dry weights [Akbour *et al.*, 2002].

### 2.3. Batch Experiments

[14] A mixture of 10 mg kaolinite mineral and 20 mL *P. putida* solution of ddH<sub>2</sub>O containing bacteria concentration from 26 to 220 mg bacteria/L was prepared. The mixture was adjusted to pH = 7 by adding appropriate amounts of 0.1 M NaOH and 0.1 M HNO<sub>3</sub> solution, and it was gently shaken (100 rpm) at 26°C  $\pm$  1°C for 120 min. Preliminary experiments showed that maximum attachment of *P. putida* onto minerals occurred within 80 min, and subsequently, no significant increase in attachment was observed. Therefore, the time duration of 120 min was considered sufficient for reaching equilibrium. Then, 3 mL of Histodenz solution (60% by weight, Sigma D2158) were injected into the suspension, as suggested by Jiang *et al.* [2007], and the mixture was centrifuged at 2500g for 4 min. Histodenz was used as density gradient separation reagent in order to separate the suspended bacteria from those attached onto kaolinite particles because the size of bacteria and kaolinite particles was of the same order.

[15] Two sets of preliminary control experiments were conducted in centrifuge tubes to determine the most appropriate conditions for the separation of suspended bacteria from bacteria attached onto kaolinite particles. In the first set, only kaolinite was placed in centrifuge tubes mixed with a cell-free solution of ddH<sub>2</sub>O and 3 mL of Histodenz solution. In the second set, only aliquots of cell cultures were transferred in centrifuge tubes mixed with a kaolinite-free solution of ddH<sub>2</sub>O and 3 mL of Histodenz solution. Initial bacteria and kaolinite concentrations were measured for each control experiment. The mixtures in tubes were centrifuged at different speeds (*g*) for various time periods. It was observed that centrifugation at 2500*g* for 4 min was optimal because for these conditions the supernatant contained all of the initial bacteria concentration and none of the kaolinite particles.

[16] The suspension of unattached bacteria in the supernatant was pipetted out and measured directly by spectrophotometry at 410 nm. The percentage of attached bacteria was determined by subtracting the mass of bacteria that remained in suspension from the initial mass of bacteria [Rong *et al.*, 2008].

[17] Histodenz is a nonionic iodinated gradient medium, which readily dissolves in water to give nontoxic, autoclavable solutions. Histodenz should be avoided if the analysis involves spectrophotometric measurements in the ultraviolet range because the attachment spectrum shows a maximum at 244 nm [Rickwood *et al.*, 1982]. To assess whether Histodenz interfered with the bacteria measurements of the present study, the absorbance of standard samples was measured at the appropriate wavelength, and it was found that the linearity of the standard curve was not affected. To our knowledge, Histodenz has never been reported in the literature to affect the surface properties of bacteria or their attachment onto solid surfaces. Also, it should be noted that the batch experiments presented in this work were conducted according to the methods and procedures employed by Jiang *et al.* [2007] and Rong *et al.* [2008], who have performed very similar experiments but with a different strain of *P. putida* and kaolinite of slightly different chemical composition.

#### 2.4. Column Experiments

[18] Flow-through experiments were conducted using a glass column with a diameter of 2.5 cm and a length of

30 cm, packed with spherical glass beads with 2 mm diameter. The column was packed with glass beads under standing ddH<sub>2</sub>O to minimize air entrapment. Screens at the inlet and outlet ends of the column held the glass beads in place and distributed the inflow evenly. The estimated dry bulk density was 1.61 g/cm<sup>3</sup>, and the porosity was 0.42. The pore volume (PV) of the column was estimated to be 61.5 mL. The entire packed column, as well as all of the glassware and materials used for the experiments, was sterilized in an autoclave at 121°C for 20 min. The column was placed horizontally. A fresh column was packed for each experiment. Also, 3 PV of ddH<sub>2</sub>O were passed through the column prior to each flow-through experiment. A schematic diagram of the experimental apparatus employed in this work is shown in Figure 1.

[19] Following the procedure outlined by Tong *et al.* [2005], the glass beads were first rinsed sequentially with acetone and hexane and then soaked in concentrated HCl for about 12 h. Next, the beads were rinsed with ddH<sub>2</sub>O until the water conductivity, as determined by a conductivity meter, was negligible. Subsequently, the glass beads were soaked in 0.1 M NaOH for 12 h and rinsed repeatedly with ddH<sub>2</sub>O until the ionic strength (IS) of water was negligible. Finally, the glass beads were dried in an oven at 105°C.

[20] Sterile ddH<sub>2</sub>O purified to a specific conductance of 0.05 μS/cm with a Milli-Q UV plus water purification system containing a UV sterilization lamp (Millipore Corp., Massachusetts) was transferred from a flask into the column with a peristaltic pump. The water flow rates employed were 2, 3, and 4 mL/min, which correspond to interstitial water velocities of  $U = q/\theta = 0.98, 1.46, \text{ and } 1.95 \text{ cm/min}$ , respectively, where  $q$  is the Darcian flux and  $\theta$  is the porosity. Throughout the experiments, the pH was maintained at 7, and the temperature was maintained at 26°C ± 1°C.

[21] Chloride, in the form of potassium chloride, was chosen as the nonreactive tracer for the characterization of the packed column. The nonreactive tracer solution (4 mS/cm) was prepared with 0.1 M KCl (12 mS/cm) in ddH<sub>2</sub>O. Preliminary experiments showed that for the relatively high flow rates used in this work, no significant gravity effects occurred in the packed column.

[22] The tracer breakthrough experiments were performed by injecting into the column 123 mL (2 PV) of 1524 mg/L Cl<sup>-</sup> solution, followed by 3 PV of ddH<sub>2</sub>O.

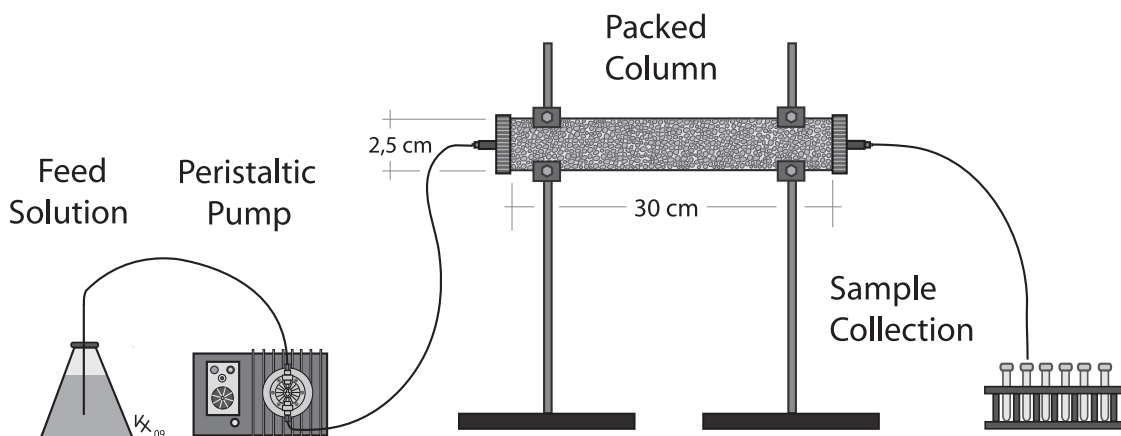
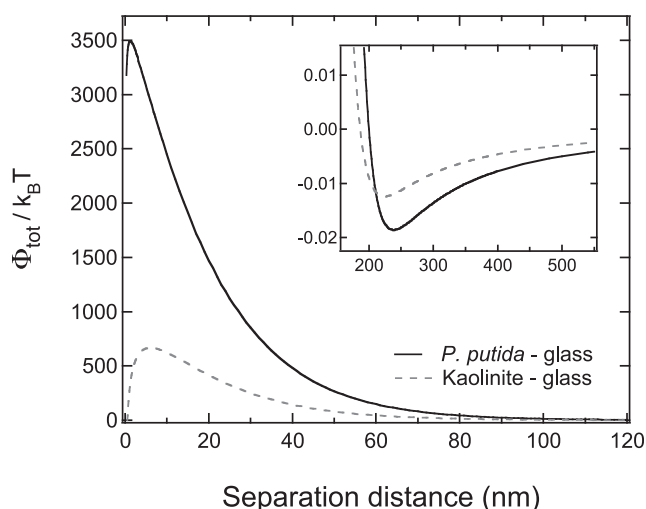


Figure 1. Schematic drawing of the experimental apparatus.

Effluent samples were collected into borosilicate test tubes. Chloride concentrations were measured using ion chromatography (DIONEX500, Sunnyvale, California). A set of flow-through experiments were performed with bacteria and kaolinite alone to understand their individual transport characteristics. For the bacterial and kaolinite transport experiments, 2 PV of colloid suspension was injected into the packed column, followed by 3 PV of ddH<sub>2</sub>O. Each experiment was performed three times to ensure reproducibility. Bacteria and kaolinite concentrations in the effluent samples were measured by spectrophotometry.

[23] The glass beads were too large for direct measurement of their zeta potential by the zeta potential analyzer. Therefore, a few glass beads were crushed into a fine powder and then mixed with ddH<sub>2</sub>O to form a sufficiently stable suspension that could be used for zeta potential measurement [Stephan and Chase, 2001]. The zeta potential of glass beads stored in ddH<sub>2</sub>O at pH 7 was determined to be  $-54.6 \pm 2.4$  mV. Subsequently, Derjaguin-Landau-Verwey-Overbeek (DLVO) interaction energies between *P. putida* and glass beads and between kaolinite and glass beads were calculated for the experimental conditions by using the measured zeta potentials, following the methodology outlined by Syngouna and Chrysikopoulos [2010]. Energy profiles for interaction between both *P. putida* and kaolinite with glass beads were constructed and are shown in Figure 2. High repulsive potentials exist between both *P. putida* and kaolinite. However, both *P. putida* and kaolinite exhibit a secondary energy minimum (see inset in Figure 2). Secondary energy minima for similar cases have also been reported in the literature [Redman et al., 2004]. Therefore, although *P. putida*, kaolinite, and glass beads all have negative surface charge under experimental conditions,



**Figure 2.** Calculated total interaction energy profiles for *P. putida* and kaolinite with glass beads as a function of separation distance for the experimental conditions. The inset highlights the corresponding secondary energy minima. Here  $\Phi_{\text{tot}}$  (J) is the total intersurface potential energy and equals the sum of the van der Waals, double-layer, and Born potential energies,  $k_B$  is Boltzmann's constant (J/K), and  $T$  (K) is temperature.

*P. putida* and kaolinite are expected to attach onto glass beads at the secondary energy minima.

## 2.5. Determination of Bacteria Attached Onto Kaolinite

[24] For the separation of bacteria attached onto kaolinite from bacteria suspended in the liquid phase, 3 mL of the column effluent were placed into 5 mL centrifuge tubes together with 0.45 mL of Histodenz solution. The mixture was centrifuged at 2500g for 4 min. The supernatant was used to determine, by spectrophotometry (410 nm), the bacteria in the liquid phase. The pellet containing the kaolinite with the attached bacteria was diluted to 3 mL as the initial volume of the sample. An aliquot (100  $\mu$ L) of the above sample was used to enumerate the bacteria attached onto kaolinite by plate counts on nutrient agar using dilution series. The total bacteria concentration in each effluent sample was estimated by adding the bacteria attached onto the kaolinite and the bacteria suspended in the aqueous phase. In addition, aliquots (100  $\mu$ L) of the effluent samples collected were analyzed for total bacteria concentration (suspended and attached) by plate counts on nutrient agar using dilution series. Effluent samples were passed through preweighed membrane filters (0.45  $\mu$ m pore size) in order to estimate the total dry weight (bacteria and kaolinite). The concentration of kaolinite was determined by subtracting the mass of bacteria (suspended and attached) from the total mass in the effluent sample.

## 2.6. SEM Images

[25] After the completion of the transport and cotransport flow-through experiments, the glass beads in the column were checked for deposited colloid particles by SEM analysis (JSM 6300, JEOL Scanning Microscope, at 20 kV). The beads were gently washed (without shaking) with few drops of ddH<sub>2</sub>O and air-dried under a fume hood [Choi et al., 2007]. Note that gentle washing of the glass beads does not affect the attached colloid particles, which remained on the surfaces of the glass beads even after flushing the packed column with 3 PV of ddH<sub>2</sub>O at the end of each flow-through experiment. The beads were mounted on aluminum stubs with carbon tape and then coated using a gold ion sputter coater (JEOL, JFC1100 Fine Coat). SEM micrographs were taken at a magnification of 6000–11,000X.

## 3. Mathematical Modeling

### 3.1. Transport

[26] The transport of the tracer, bacteria, and clay in homogeneous, water-saturated porous media, assuming negligible growth and decay, is governed by the following partial differential equation [Sim and Chrysikopoulos, 1995]:

$$\frac{\partial C_i}{\partial t} + \frac{\rho_m}{\theta} \frac{\partial C_i^*}{\partial t} = D_i \frac{\partial^2 C_i}{\partial x^2} - U \frac{\partial C_i}{\partial x} \quad (1)$$

$$\frac{\rho_m}{\theta} \frac{\partial C_i^*}{\partial t} = r_{i-t} C_i - \frac{\rho_m}{\theta} r_{i-c} C_i^* \quad (2)$$

where the subscript  $i$  is  $t$  (tracer),  $b$  (bacteria), or  $c$  (clay),  $C_i$  (mg of  $i/\text{cm}^3$ ) is the concentration of species  $i$  dissolved or suspended in the aqueous phase,  $C_i^*$  (mg of  $i/\text{mg}$  solids)

is the concentration of species  $i$  attached onto the solid phase,  $U$  is the interstitial velocity (cm/min),  $\rho_m$  (mg solids/cm<sup>3</sup> solid matrix) is the bulk density of the solid matrix,  $\theta$  (cm<sup>3</sup> voids/cm<sup>3</sup> solid matrix) is the porosity of the column material,  $t$  (min) is time,  $r_{i-i^*}$  (1/min) is the attachment (deposition) rate coefficient of species  $i$  onto glass beads,  $r_{i^*-i}$  (1/min) is the detachment rate coefficient of species  $i$  from glass beads, and  $D_i$  (cm<sup>2</sup>/min) is the hydrodynamic dispersion coefficient defined as [Bear, 1979]

$$D_i = \alpha_L U + D_{e_i}, \quad (3)$$

where  $\alpha_L$  (cm) is the longitudinal dispersivity and  $D_{e_i}$  (cm<sup>2</sup>/min) is the effective diffusion coefficient of species  $i$ . For the experimental conditions of the present study, the appropriate initial and boundary conditions are

$$C_i(0, x) = 0 \quad (4)$$

$$C_i(t, 0) = \begin{cases} C_{i_0} & t \leq t_p \\ 0 & t > t_p \end{cases} \quad (5)$$

$$\frac{\partial C_i(t, L)}{\partial x} = 0, \quad (6)$$

where  $t_p$  (min) is the injection time period,  $C_{i_0}$  (mg of  $i$ /cm<sup>3</sup>) is the initial aqueous phase concentration of species  $i$ , and  $L$  (cm) is the column length. The condition (4) establishes that there is no initial bacteria concentration within the one-dimensional porous medium. The first-type boundary condition (5) implies constant concentration at the inlet over the injection time period. The downstream boundary condition (6) preserves the concentration continuity at the outlet of the column.

### 3.2. Cotransport

[27] It is assumed that clay particles partition between the aqueous phase and the solid matrix, while bacteria partition onto clay surfaces and the solid matrix. Thus, clay particles can be suspended in the aqueous phase or attached onto the solid matrix. Bacteria can be suspended in the aqueous phase, directly attached onto the solid matrix, attached onto suspended clay surfaces, and attached onto clay particles that are already attached onto the solid matrix. Furthermore, assuming negligible bacteria chemotaxis, growth, and decay, the governing cotransport equations for one-dimensional, homogeneous, water-saturated porous media are given by equation (1) and (2) for the transport of clay particles together with the following mass balance equation for bacteria suspended in the aqueous phase [Abdel-Salam and Chrysiopoulos, 1995a, 1995b] (accumulation = dispersion – advection):

$$\begin{aligned} \frac{\partial}{\partial t} \left[ C_b + \frac{\rho_m}{\theta} C_b^* + C_c C_{bc} + \frac{\rho_m}{\theta} C_c^* C_{bc}^* \right] &= D_b \frac{\partial^2 C_b}{\partial x^2} + D_{bc} \frac{\partial^2}{\partial x^2} [C_c C_{bc}] \\ &\quad - U \frac{\partial}{\partial x} [C_b + C_c C_{bc}], \end{aligned} \quad (7)$$

where  $C_{bc}$  (mg bacteria/mg clay) is the concentration of bacteria attached onto suspended clay particles, or “sus-

pended bacteria-clay particles”;  $C_{bc}^*$  (mg bacteria/mg clay) is the concentration of bacteria attached onto clay particles already attached onto glass beads, or “attached bacteria-clay particles”; and  $D_{bc}$  (cm<sup>2</sup>/min) is the hydrodynamic dispersion coefficient for suspended bacteria-clay particles. The second mass accumulation rate on the left side of equation (7) is given by equation (2), and the third rate is expressed as [Bekhit *et al.*, 2009]

$$\frac{\partial (C_c C_{bc})}{\partial t} = \Lambda_{b-bc} - \Lambda_{bc-b} + \Lambda_{b^*c^*-bc} - \Lambda_{bc-b^*c^*}, \quad (8)$$

where  $\Lambda_{b-bc}$  (mg bacteria/(cm<sup>3</sup> min)) is the mass accumulation rate due to attachment of suspended bacteria onto suspended clay particles, expressed by the following pseudo-second-order rate law:

$$\Lambda_{b-bc} = r_{b-bc} (C_{bc_{eq}} - C_{bc})^2 C_c, \quad (9)$$

where  $r_{b-bc}$  (mg clay/(mg bacteria min)) is the attachment rate coefficient of suspended bacteria onto suspended clay particles and  $C_{bc_{eq}}$  (mg bacteria/mg clay) is the concentration of bacteria attached onto suspended clay particles at equilibrium.  $\Lambda_{bc-b}$  (mg bacteria/(cm<sup>3</sup> min)) is the mass accumulation rate due to bacteria detachment from suspended clay particles, expressed by the following relationship:

$$\Lambda_{bc-b} = r_{bc-b} (C_c C_{bc}), \quad (10)$$

where  $r_{bc-b}$  (1/min) is the rate coefficient for bacteria detachment from suspended clay particles.  $\Lambda_{bc-b^*c^*}$  (mg bacteria/(cm<sup>3</sup> min)) is the mass accumulation rate due to attachment of suspended bacteria-clay particles (bacteria attached onto suspended clay particles) onto glass beads, expressed as

$$\Lambda_{bc-b^*c^*} = r_{bc-b^*c^*} (C_c C_{bc}), \quad (11)$$

where  $r_{bc-b^*c^*}$  (1/min) is the attachment rate coefficient of suspended bacteria-clay particles onto glass beads.  $\Lambda_{b^*c^*-bc}$  (mg bacteria/(cm<sup>3</sup> min)) is the mass accumulation rate due to detachment of attached bacteria-clay particles (bacteria attached onto clay particles already attached onto glass beads) from glass beads, expressed by the following relationship:

$$\Lambda_{b^*c^*-bc} = \frac{\rho_m}{\theta} r_{b^*c^*-bc} (C_c^* C_{bc}^*), \quad (12)$$

where  $r_{b^*c^*-bc}$  (1/min) is the detachment rate coefficient of bacteria-clay particles from glass beads.

[28] The fourth mass accumulation rate on the left side of equation (7) is expressed as [Bekhit *et al.*, 2009]

$$\frac{\rho_m}{\theta} \frac{\partial (C_c^* C_{bc}^*)}{\partial t} = \Lambda_{b-b^*c^*} - \Lambda_{b^*c^*-b} + \Lambda_{bc-b^*c^*} - \Lambda_{b^*c^*-bc}, \quad (13)$$

where  $\Lambda_{b-b^*c^*}$  (mg bacteria/(cm<sup>3</sup> min)) is the mass accumulation rate due to attachment of suspended bacteria onto clay particles already attached onto glass beads, expressed by the following pseudo-second-order rate law:

$$\Lambda_{b-b^*c^*} = \frac{\rho_m}{\theta} r_{b-b^*c^*} (C_{bc_{eq}}^* - C_{bc}^*)^2 C_c^* \quad (14)$$

where  $r_{b-b^*c^*}$  (mg clay/(mg bacteria min)) is the attachment rate coefficient of suspended bacteria onto clay particles already attached onto glass beads and  $C_{bc_{eq}}^*$  (mg bacteria/mg clay) is the concentration of bacteria attached onto clay particles already attached onto glass beads at equilibrium.  $\Lambda_{b^*c^*-b}$  (mg bacteria/(cm<sup>3</sup> min)) is the mass accumulation rate due to detachment of bacteria from clay particles attached onto glass beads, expressed by the following relationship:

$$\Lambda_{b^*c^*-b} = \frac{\rho_m}{\theta} r_{b^*c^*-b} (C_c^* C_{bc}^*), \quad (15)$$

where  $r_{b^*c^*-b}$  (1/min) is the rate coefficient of bacteria detachment from clay particles attached onto glass beads. The numerical solution of the model partial differential equations and the fitting of the model to the various breakthrough data sets were obtained with the commercial numerical code Aquasim (version 2.1d), which uses a fully implicit finite difference spatial discretization scheme [Gear, 1971] in conjunction with the algorithm DASSL [Petzold, 1983].

### 3.3. Moment Analysis

[29] The concentration breakthrough curves of concentration  $C(x,t)$  obtained at location  $x = L$  were analyzed by the normalized absolute moments, which are defined as

$$M_n(x) = \frac{\int_0^\infty t^n C_i(x,t) dt}{\int_0^\infty C_i(x,t) dt} \quad (16)$$

[30] The first normalized temporal moment,  $M_1$ , characterizes the center of mass of the concentration breakthrough curve and defines the mean breakthrough time or average velocity. The second normalized temporal moment,  $M_2$ , characterizes the spreading of the breakthrough curve. Furthermore, the mass recovery,  $M_r$ , of the tracer or suspended particles is quantified by the following expression:

$$M_r(L) = \frac{m_0(L)}{C_{i0} t_p} = \frac{\int_0^\infty C_i(L,t) dt}{\int_0^{t_p} C_i(0,t) dt} \quad (17)$$

where  $m_0$  is the zeroth absolute moment and quantifies the total mass in the concentration breakthrough curve.

## 4. Results

### 4.1. Batch Experiments

[31] The data from the batch equilibrium experiments of *P. putida* attachment onto kaolinite are shown in Figure 3, and they were fitted with a Langmuir type isotherm:

$$C_{bc_{eq}} = \frac{Q^\circ \alpha_1 C_{bc_{eq}}}{1 + \alpha_1 C_{bc_{eq}}}, \quad (18)$$

where  $Q^\circ = 94.6$  (mg bacteria/g clay) is the fitted maximum amount of bacteria that may be attached onto kaolinite,  $\alpha_1 = 0.0095$  (L/mg bacteria) is a fitted constant related to the attachment energy, and  $C_{bc_{eq}}$  (mg bacteria/L) is the

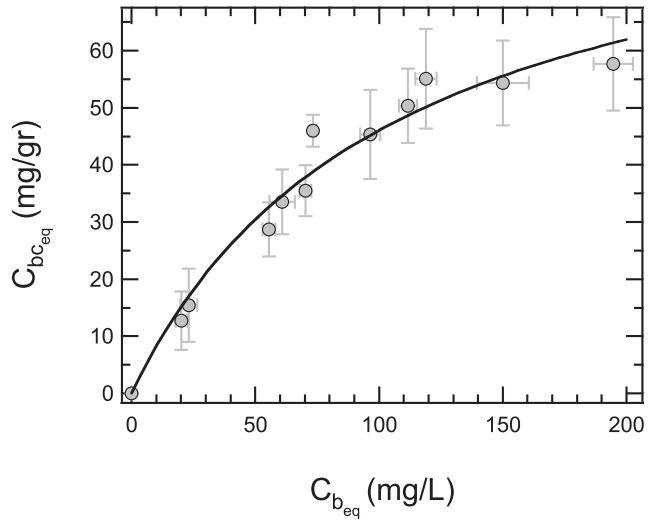


**Figure 3.** Equilibrium attachment data of *P. putida* onto kaolinite (circles) and fitted Langmuir isotherm (curve).

liquid phase concentration of bacteria at equilibrium, which ranged from 20 to 195 mg/L. Similar attachment behavior has been observed by Jiang *et al.* [2007] for attachment of *P. putida* onto kaolinite, goethite, and montmorillonite. Furthermore, to investigate the kinetics of *P. putida* attachment onto kaolinite, additional batch experiments were conducted, and the data are shown in Figure 4. The kinetic experimental data indicate that equilibrium was reached at approximately 80 min. Furthermore, the kinetic data were adequately fitted by the following pseudo-second-order rate law [Ho *et al.*, 2001; Upadhyayula *et al.*, 2009]:

$$\frac{dC_{bc}}{dt} = r_{b-bc} (C_{bc_{eq}} - C_{bc})^2 \quad (19)$$

[32] The fitted parameters ( $r_{b-bc}$ ,  $C_{bc_{eq}}$ ) for the three initial *P. putida* concentrations examined and the liquid phase

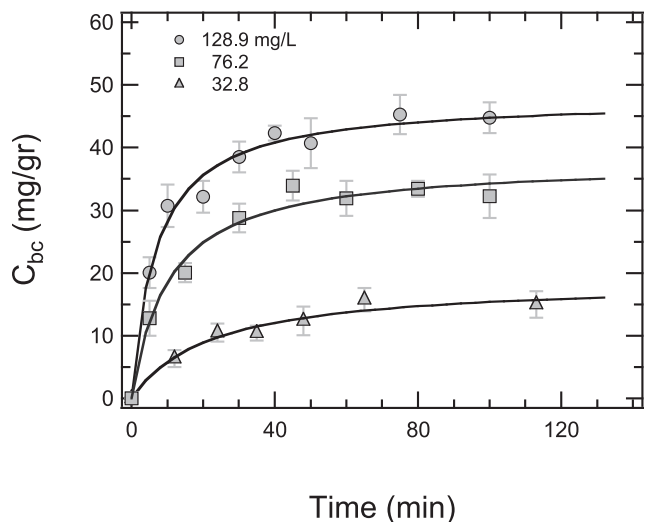


**Figure 4.** Attachment kinetics of *P. putida* onto kaolinite for three different initial bacteria concentrations (symbols) and fitted pseudo-second-order model (curves).

**Table 1.** Fitted Parameters Obtained From *P. putida* Attachment Kinetic Experiments

Initial <i>P. putida</i> Concentration (mg/L)	$C_{bc_{eq}}$ (mg bacteria/g clay)	$C_{bc_{eq}}$ Experimental (mg bacteria/L)	$r_{b-bc}$ ( $\times 10^{-2}$ g clay/mg bacteria min)
32.8	$18.8 \pm 1.7$	$25.1 \pm 0.3$	$0.24 \pm 0.08$
76.2	$37.8 \pm 1.4$	$59.6 \pm 0.4$	$0.25 \pm 0.05$
128.9	$47.8 \pm 1.4$	$106.2 \pm 0.3$	$0.30 \pm 0.05$

bacteria concentrations at equilibrium ( $C_{bc_{eq}}$ ) for the sorption kinetic experiments are listed in Table 1. Note that  $r_{b-bc}$  and  $C_{bc_{eq}}$  increased with increasing initial *P. putida* concentration  $C_{b_0}$ .

#### 4.2. Transport Experiments

[33] The normalized chloride breakthrough data together with the *P. putida* data are presented in Figures 5a–5c, and the kaolinite data are presented in Figures 5d–5f for three different interstitial velocities and various initial concentrations. The corresponding  $M_r$  values are calculated using equation (17) and are listed in Table 2. The break-

through data for  $Cl^-$  and *P. putida* have similar shapes without any tailing effects, indicating that there was no significant retention by the packed column. This observation is consistent with the  $M_r$  estimated for both  $Cl^-$  and *P. putida*, except for *P. putida* for  $U = 0.98$  cm/min, which yielded  $M_r = 99.4\%$  (see Table 2). The slight attachment of *P. putida* onto glass beads was also verified by SEM analysis (see Figure 6a), and it was attributed to the low  $U$ . Note that  $U = 0.98$  cm/min was the lowest velocity used. Tailing was observed in the kaolinite transport experiments, and the associated  $M_r$  values indicated that kaolinite mass retention decreased with increasing  $U$  and initial kaolinite

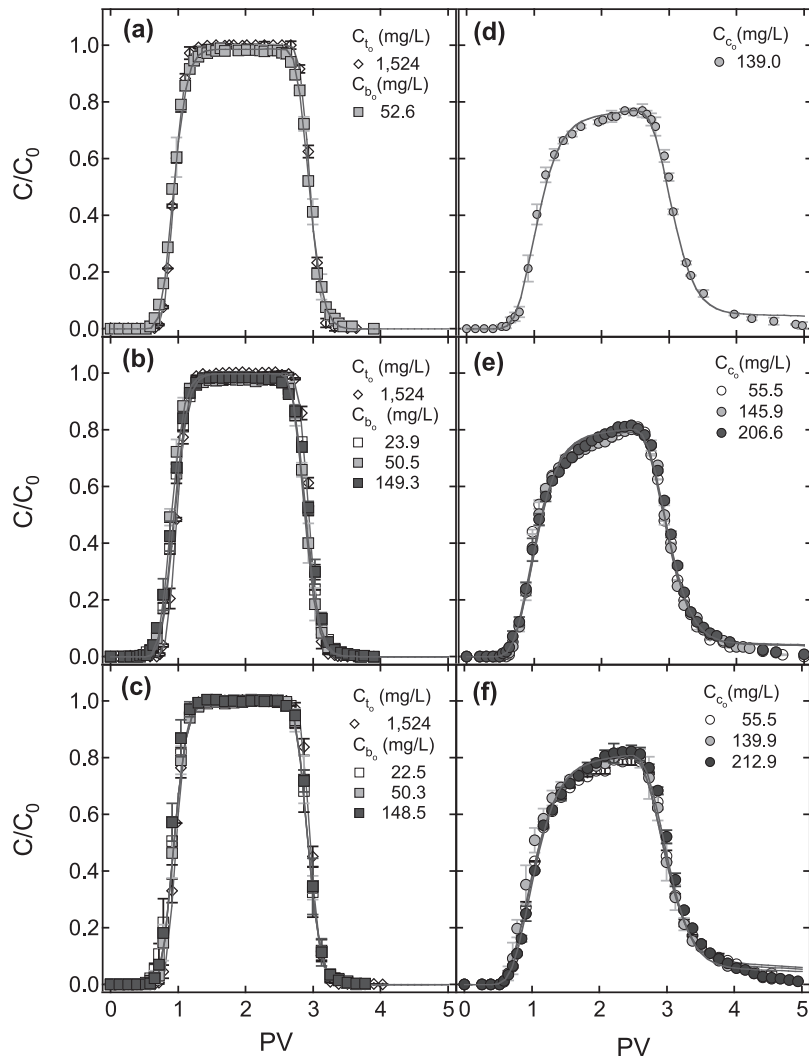


**Figure 5.** Experimental data (symbols) and fitted model simulations (curves) for transport of chloride and bacteria with  $U$  equal to (a) 0.98, (b) 1.46, and (c) 1.95 cm/min and transport of kaolinite with  $U$  equal to (d) 0.98, (e) 1.46, and (f) 1.95 cm/min.

**Table 2.** Mass Recoveries and Model Parameters for Chloride, *P. putida*, and Kaolinite Transport Experiments

Initial Concentration (mg/L)	$U$ (cm/min)	$M_r$ (%)	$D_i$ (cm <sup>2</sup> /min)	$\alpha_L$ (cm)	$r_{b-b^*}$ ( $\times 10^{-3}$ 1/min)	$r_{b^*-b}$ ( $\times 10^{-3}$ 1/min)	$r_{c-c^*}$ ( $\times 10^{-3}$ 1/min)	$r_{c^*-c}$ ( $\times 10^{-3}$ 1/min)	$M_{1(g)}/M_{1(t)}$
<b>Cl<sup>-</sup> (<math>C_0</math>)</b>									
1524	0.98	101.1 $\pm$ 0.3	0.25 $\pm$ 0.01	0.26 $\pm$ 0.01					1.00
1524	1.46	101.3 $\pm$ 0.6	0.37 $\pm$ 0.01	0.25 $\pm$ 0.01					1.00
1524	1.95	102.5 $\pm$ 0.3	0.42 $\pm$ 0.04	0.22 $\pm$ 0.03					1.00
<b><i>P. putida</i> (<math>C_{b_0}</math>)</b>									
52.6	0.98	99.4 $\pm$ 1.0	0.44 $\pm$ 0.02	0.45 $\pm$ 0.03	0.16 $\pm$ 0.08	0.19 $\pm$ 0.01			1.00
23.9	1.46	101.1 $\pm$ 0.5	0.68 $\pm$ 0.02	0.47 $\pm$ 0.02	0.32 $\pm$ 0.09	0.92 $\pm$ 0.02			0.98
50.5	1.46	101.0 $\pm$ 0.6	0.67 $\pm$ 0.05	0.46 $\pm$ 0.05	0.35 $\pm$ 0.06	1.14 $\pm$ 0.05			0.96
149.3	1.46	102.7 $\pm$ 1.0	0.68 $\pm$ 0.07	0.47 $\pm$ 0.07	0.40 $\pm$ 0.01	1.09 $\pm$ 0.17			0.98
22.5	1.95	103.2 $\pm$ 1.0	0.79 $\pm$ 0.08	0.41 $\pm$ 0.06	0.52 $\pm$ 0.01	3.83 $\pm$ 0.13			0.98
50.3	1.95	102.3 $\pm$ 0.4	0.79 $\pm$ 0.12	0.41 $\pm$ 0.09	0.55 $\pm$ 0.02	3.92 $\pm$ 0.07			0.98
148.5	1.95	102.5 $\pm$ 0.8	0.80 $\pm$ 0.15	0.41 $\pm$ 0.11	0.54 $\pm$ 0.09	3.89 $\pm$ 0.05			0.98
<b>Kaolinite (<math>C_{c_0}</math>)</b>									
139.0	0.98	81.4 $\pm$ 0.9	1.01 $\pm$ 0.06	1.03 $\pm$ 0.09			9.41 $\pm$ 0.11	4.54 $\pm$ 0.92	1.11
55.5	1.46	83.1 $\pm$ 0.5	1.59 $\pm$ 0.12	1.09 $\pm$ 0.11			12.89 $\pm$ 0.24	7.41 $\pm$ 0.25	1.06
145.9	1.46	83.0 $\pm$ 0.5	1.57 $\pm$ 0.13	1.07 $\pm$ 0.12			12.69 $\pm$ 0.41	6.53 $\pm$ 0.11	1.07
206.6	1.46	85.2 $\pm$ 0.5	1.61 $\pm$ 0.11	1.10 $\pm$ 0.11			12.13 $\pm$ 0.45	7.06 $\pm$ 0.92	1.08
55.5	1.95	84.8 $\pm$ 0.5	2.38 $\pm$ 0.28	1.22 $\pm$ 0.20			18.77 $\pm$ 0.70	17.03 $\pm$ 1.02	1.10
139.9	1.95	88.2 $\pm$ 1.5	2.35 $\pm$ 0.26	1.20 $\pm$ 0.19			17.68 $\pm$ 0.83	17.80 $\pm$ 0.52	1.07
212.9	1.95	87.8 $\pm$ 0.4	2.24 $\pm$ 0.20	1.15 $\pm$ 0.15			18.06 $\pm$ 0.72	18.90 $\pm$ 1.20	1.11

concentration  $C_{c_0}$ . As shown in the SEM image of Figure 6b, it is evident that kaolinite particles were attached onto glass beads.

[34] The transport model was fitted to the chloride, *P. putida*, and kaolinite experimental data. For the chloride data, only one parameter ( $D_i$ ) was fitted. For the *P. putida* data, there were three fitted parameters ( $D_b$ ,  $r_{b-b^*}$ , and  $r_{b^*-b}$ ). Also, there were three fitted parameters ( $D_c$ ,  $r_{c-c^*}$ ,

and  $r_{c^*-c}$ ) for the kaolinite data. All fitted parameters are listed in Table 2. The fitted model simulations were plotted together with the corresponding experimental data in Figure 5. All model simulations were in very good agreement with the experimental data.

[35] Assuming that the effective diffusion coefficient  $D_e$  (cm<sup>2</sup>/min) was negligible compared to the product  $\alpha_L U$ , equation (3) was employed to estimate the various

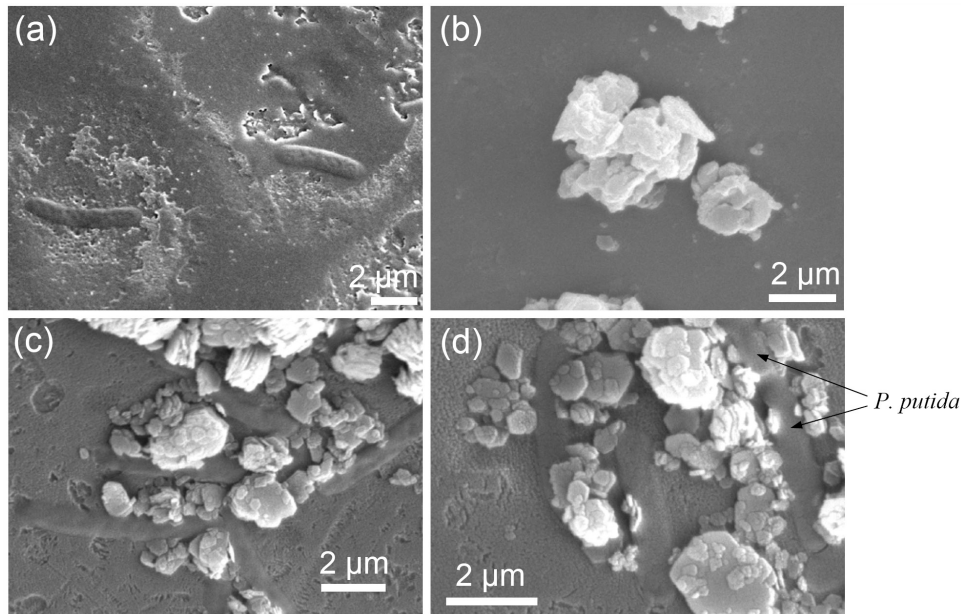


**Figure 6.** Scanning electron microscopy images of (a) *P. putida* deposited on a glass bead of the packed column for the transport experiment with  $U = 0.98$  cm/min, (b) kaolinite particles deposited on a glass bead for the transport experiment with  $U = 1.95$  cm/min, (c) *P. putida*–kaolinite particles attached onto a glass bead, and (d) *P. putida*–kaolinite particles attached onto a glass bead and *P. putida* probably attached onto kaolinite previously attached onto a glass bead (see top right corner) during cotransport at  $U = 1.95$  cm/min.

dispersivities, which are listed in Table 2. The very small variability in the estimated  $\alpha_L$  values observed for each set of transport experiments conducted with  $\text{Cl}^-$ , *P. putida*, and kaolinite verified that the columns were consistently uniformly packed. The estimated  $\alpha_L$  values were higher for kaolinite than for *P. putida*. Although the mean kaolinite diameter varied, it was smaller than the equivalent diameter of *P. putida*. Therefore, it was evident that  $\alpha_L$  for suspended colloid particles is not just a property of the porous medium but also depends on colloid size and decreases with increasing particle size. Similar results are reported by Keller et al. [2004].

[36] The fitted attachment and detachment rate coefficients for both *P. putida* and kaolinite are listed in Table 2, and they increase with increasing  $U$ . Note that consistently  $r_{b-b^*} < r_{b^*-b}$  and  $r_{c-c^*} \geq r_{c^*-c}$ . Higher attachment and detachment rate coefficients have also been observed for *E. coli* transport in porous media because of the existence of a secondary energy minimum [Smith et al. 2008]. It is worth noting that as the attachment and detachment rate coefficients increased with increasing flow rate, the ratio of attachment to detachment rate coefficients decreased with increasing flow rate. For both *P. putida* and kaolinite, the attachment and detachment rate coefficients increased with increasing flow rate, but the ratio of attachment to detachment rate coefficients decreased with increasing flow rate. A possible explanation for this is that because of the existence of a secondary energy minimum, hydrodynamics had greater influence on the detachment than the attachment process. However, additional work is needed to verify this. Straining cannot be considered an important mechanism of mass loss in the physical system examined in this study because the average size of the bacteria cells ( $2.16 \pm 0.44 \mu\text{m}$ ) and kaolinite particles ( $<2 \mu\text{m}$ ) were approximately  $\sim 0.1\%$  of the average diameter of glass beads (2 mm), which were much smaller than the 5% limit recommended by Hendry et al. [1999] and Choi et al. [2007] or the 0.5% limit recommended by Bradford et al. [2004].

[37] The first moment (average velocity) was calculated with equation (16) for each breakthrough curve. Also, for each  $U$  employed, the first normalized temporal moment  $M_{1(i)}$  ratio of the two colloids (*P. putida* and kaolinite) to  $M_{1(i)}$  for the tracer  $\text{Cl}^-$  was computed and is listed in Table 2. A ratio  $M_{1(i)}/M_{1(i)} > 1$  denotes that colloid velocity is retarded, whereas a ratio smaller than 1 denotes that the colloid velocity is enhanced. The results from Table 2 indicated that the mean velocity of *P. putida* was very slightly enhanced (0%–4%) and the mean velocity of kaolinite was significantly retarded (6%–11%) compared to the  $\text{Cl}^-$  movement.

### 4.3. Cotransport Experiments

[38] The normalized *P. putida* and kaolinite cotransport breakthrough data are presented in Figure 7 for two different interstitial velocities. Two different initial concentrations for *P. putida* and kaolinite were employed. The suspended *P. putida* breakthrough concentrations were labeled as  $C_b$ , the total *P. putida* concentrations (suspended plus attached onto kaolinite) were labeled as  $C_b + C_{bc}$ , and the total *P. putida* concentrations measured by plate counts on nutrient agar were labeled as  $C_{\text{Total}-b}$ . The  $C_b$ ,  $C_b + C_{bc}$ , and  $C_{\text{Total}-b}$  breakthrough data for the four cotransport

experiments conducted are presented in Figures 7a, 7c, 7e, and 7g. The suspended kaolinite breakthrough concentrations were labeled as  $C_c$ , and the concentrations of *P. putida* attached onto suspended kaolinite were labeled as  $C_{bc}$ . The  $C_c$  and  $C_{bc}$  data for the four cotransport experiments conducted are presented in Figures 7b, 7d, 7f, and 7h. The corresponding  $M_r$  values were calculated using (17), and they are listed in Table 3.

[39] The experimental data show that kaolinite affected the transport of *P. putida* through the glass bead packs. The  $M_r$  of total *P. putida* was reduced in the presence of kaolinite particles (see Table 3) compared to the case of *P. putida* transport in the absence of kaolinite (see Table 2).

[40] The observed reduction in  $C_b$  was attributed to (1) attachment of suspended bacteria onto suspended kaolinite particles to form suspended bacteria-kaolinite particles ( $C_{bc}$ ), which in turn could be retained by the solid matrix, and (2) attachment of suspended bacteria onto kaolinite already attached onto the glass beads. Figures 6c and 6d show various bacteria-kaolinite particles attached onto glass bead surfaces. It is worth noting the upper right corner of Figure 6d, where a bacterium cell is lying onto kaolinite particles, which appear to have been attached onto the glass bead prior to the adhesion of the bacterium. Also, it should be noted that for the experimental conditions of the SEM images in Figures 6c and 6d ( $U = 1.95 \text{ cm/min}$ ), no *P. putida* attachment onto glass beads was observed in the absence of kaolinite and  $M_r$  was estimated to be 100% (see Table 2).

[41] The data from the cotransport experiments shown in Figure 7 together with the parameter values listed in Table 3 indicate that the  $M_r$  of *P. putida* decreased with increasing the initial kaolinite concentration  $C_{c0}$  (mg/L) because of increased kaolinite attachment onto the solid matrix, which in turn led to additional favorable positions for suspended *P. putida* to attach. Decreasing the initial bacteria concentration  $C_{b0}$  (mg/L) resulted in higher  $C_{bc}$  and lower  $C_b$  effluent concentrations. Lowering  $U$  resulted in reduced  $M_r$  of *P. putida* because of the increased retention time, which in turn led to enhanced attachment of suspended *P. putida* onto suspended and attached kaolinite particles. Also, the presence of *P. putida* affected kaolinite transport because the  $M_r$  of kaolinite was substantially reduced in the presence of *P. putida* (see Table 3) compared to the case of kaolinite transport in the absence of *P. putida* (see Table 2). Furthermore, the various ratios  $M_{1(i)}/M_{1(i)}$  listed in Table 3 indicate that mean velocity of *P. putida* was very slightly enhanced (0%–3%) and the mean velocity of kaolinite was significantly retarded (3%–11%) compared to the  $\text{Cl}^-$  movement.

[42] The dispersion coefficients for bacteria and kaolinite particles have the same values as those obtained from the individual flow-through experiments (see Table 2). Assuming that  $C_{bc}$  and  $C_c$  exhibited identical fate and transport characteristics ( $D_{bc} = D_c$ ,  $r_{bc-b^*c^*} = r_{c-c^*}$ , and  $r_{b^*c^*-bc} = r_{c^*-c}$ ), the various fitted attachment and detachment rate coefficients for the cotransport experiments are listed in Table 3. It was observed that  $r_{bc-b}$  increased with increasing  $C_{b0}/C_{c0}$  ratio and  $U$ . Increasing  $r_{bc-b}$  enhanced the  $M_r$  of  $C_b$ . The fitted model simulations are plotted together with the corresponding experimental data in Figure 7. Good agreement between the experimental data and the model predictions is observed.

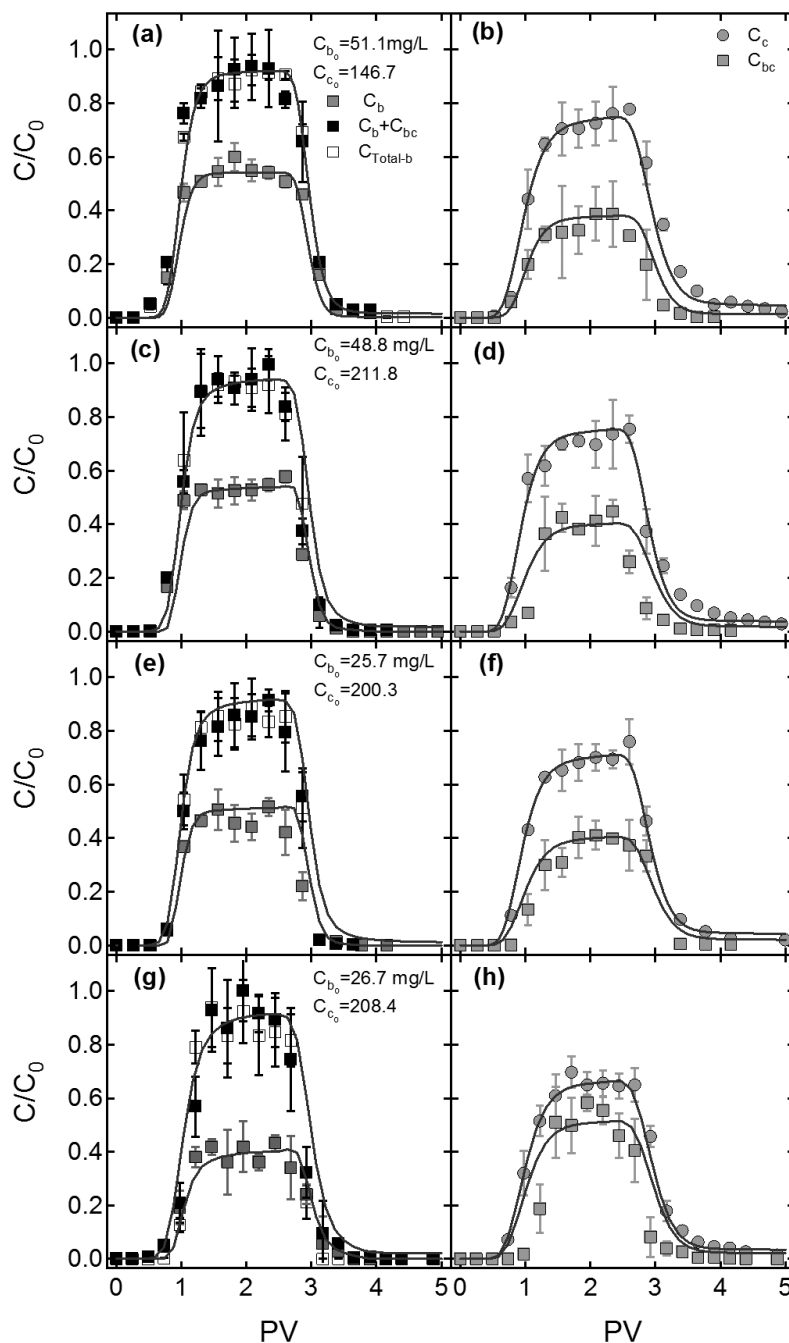


**Figure 7.** Experimental data for *P. putida* and kaolinite cotransport (symbols) and fitted models (solid curves) for various initial *P. putida* and kaolinite concentrations and interstitial velocity of (a–f)  $U = 1.95$  cm/min and (g, h)  $U = 1.46$  cm/min.

## 5. Discussion

[43] The observed increase in *P. putida* and kaolinite retention with decreasing  $U$  is in agreement with the colloid filtration theory and with previous studies [Camper *et al.*, 1993; Compere *et al.*, 2001; Akbour *et al.*, 2002; Choi *et al.*, 2007]. A decrease in  $U$  led to an increasing number of collisions between suspended particles and collectors and enhancement of particle retention. At low  $U$ , motile bacteria do not follow the colloid filtration theory because swimming cells may avoid sticking onto soil grains [Camesano

and Logan, 1998]. At the relatively high  $U$  used in this study, *P. putida* attachment was not affected by bacteria motility. Other investigators have also reported in the literature that peak aqueous phase bacteria concentrations were not affected by bacteria motility at high  $U$  [Camper *et al.*, 1993; Choi *et al.*, 2007]. However, for low  $U$ , bacteria motility could lead to early breakthrough [Camper *et al.*, 1993; Camesano and Logan, 1998].

[44] *P. putida* retention within the packed column was not affected by  $C_{b_0}$ , but kaolinite retention decreased with

**Table 3.** Mass Recoveries and Model Parameters for *P. putida*, and Kaolinite Cotransport Experiments

Initial Concentrations (mg/L)	<i>U</i> (cm/min)	<i>M<sub>r</sub></i> (%)			<i>r<sub>bc</sub></i> (mg clay/mg bacteria min)	<i>r<sub>b-c</sub></i> (mg clay/mg bacteria min)	<i>r<sub>b-c</sub></i> (mg clay/mg bacteria min)	<i>r<sub>b-c</sub></i> (1/min)	<i>r<sub>b-c</sub></i> (1/min)	<i>r<sub>b-c</sub></i> (1/min)	<i>C<sub>b,eq</sub></i> (mg bacteria/mg clay)	<i>C<sub>b,eq</sub></i> (mg bacteria/mg clay)	<i>M<sub>r</sub></i> (%)
		<i>C<sub>total-b</sub></i> , <i>C<sub>c</sub></i>	<i>C<sub>b</sub></i>	<i>C<sub>bc</sub></i>									
<i>P. putida</i> <i>C<sub>b0</sub></i> = 51.1, kaolinite <i>C<sub>c0</sub></i> = 146.7	1.95	96.4 ± 15.0, 83.1 ± 11.6	61.4 ± 4.4	34.1 ± 13.7	0.98 ± 0.07, 22.1 ± 0.3	11.80 ± 0.4, 8.27 ± 0.25	0.39 ± 0.06, 0.36 ± 0.07	0.22 ± 0.05, 0.21 ± 0.04	0.97 ± 0.09, 0.95 ± 0.08	0.022 ± 0.002, 0.069 ± 0.002	0.27 ± 0.02, 0.22 ± 0.01	0.18 ± 0.01, 0.16 ± 0.03	1.00, 1.11
<i>P. putida</i> <i>C<sub>b0</sub></i> = 48.8, kaolinite <i>C<sub>c0</sub></i> = 211.8	1.95	90.6 ± 12.5, 80.3 ± 8.4	56.4 ± 4.4	34.0 ± 8.5	0.89 ± 0.06, 22.07 ± 0.84	12.79 ± 1.0, 6.84 ± 0.92	0.39 ± 0.04, 0.39 ± 0.04	0.21 ± 0.04, 0.39 ± 0.02	0.95 ± 0.08, 0.93 ± 0.03	0.069 ± 0.002, 0.081 ± 0.003	0.22 ± 0.01, 0.15 ± 0.03	0.16 ± 0.03, 0.099 ± 0.004	0.97, 1.07
<i>P. putida</i> <i>C<sub>b0</sub></i> = 25.7, kaolinite <i>C<sub>c0</sub></i> = 200.3	1.95	84.0 ± 16.1, 74.9 ± 7.6	47.8 ± 7.6	37.9 ± 10.5	2.19 ± 0.3, 26.07 ± 0.3	3.51 ± 0.43, 6.84 ± 0.78	0.39 ± 0.04, 0.48 ± 0.02	0.39 ± 0.02, 0.40 ± 0.05	0.93 ± 0.03, 0.27 ± 0.02	0.081 ± 0.003, 0.081 ± 0.003	0.15 ± 0.03, 0.16 ± 0.02	0.099 ± 0.004, 0.099 ± 0.004	0.99, 1.03
<i>P. putida</i> <i>C<sub>b0</sub></i> = 26.7, kaolinite <i>C<sub>c0</sub></i> = 208.4	1.46	81.2 ± 16.2, 71.9 ± 10.4	41.1 ± 12.0	42.2 ± 12.8	1.11 ± 0.1, 21.39 ± 1.4	10.82 ± 1.3, 3.53 ± 0.5	0.48 ± 0.02, 0.48 ± 0.02	0.40 ± 0.05, 0.40 ± 0.05	0.27 ± 0.02, 0.27 ± 0.02	0.081 ± 0.003, 0.081 ± 0.003	0.16 ± 0.02, 0.16 ± 0.02	0.099 ± 0.004, 0.099 ± 0.004	1.00, 1.08

increasing *C<sub>c0</sub>*. Although the clean bed filtration theory does not account for suspended particle concentration [Dabros and van de Ven, 1982], high colloid concentrations are known to affect colloid retention in porous media [Rijnaarts et al., 1996; Liu et al., 1995]. The lower *M<sub>r</sub>* of kaolinite compared to that of *P. putida* (see Table 2) was attributed to the higher zeta potential of kaolinite particles (-22.5 mV) compared to *P. putida* (-44.2 mV) because the repulsive forces between negatively charged suspended particles and negatively charged glass bead surfaces increased with increasing negative charge of suspended particles. Furthermore, *P. putida* and kaolinite colloids were observed to travel faster than the conservative tracer because the sizes of *P. putida* and kaolinite particles were of similar size.

[45] Large colloids are often excluded from small pores. Consequently, size exclusion may influence the transport behavior of colloids by limiting their transport to the larger pores [Camper et al., 1993; Kretzschmar and Sticher, 1997; Chrysiopoulos and Abdel-Salam, 1997; Akbhour et al., 2002]. In addition, if the electrostatic forces between colloids and porous media are repulsive, then colloids may be excluded from locations adjacent to solid surfaces because of charge exclusion. If the colloids are excluded from pore spaces, they are likely to sample the more conductive ranges of the *U* distribution, and hence, they are transported faster than a conservative tracer [Harter et al., 2000; James and Chrysiopoulos, 2003]. The *α<sub>L</sub>* for kaolinite was greater than that of *P. putida* because smaller colloids have a more diverse path flow through columns packed with glass beads.

[46] For *P. putida* and kaolinite cotransport in a porous medium, the interactions among the two different colloids resulted in increased *M<sub>r</sub>* for both colloids compared to the *M<sub>r</sub>* for transport of each colloid separately. As *C<sub>c0</sub>* increased, *C<sub>b</sub>* decreased because more kaolinite particles attached onto the glass beads and offered more attachment positions for suspended *P. putida*. Increasing *C<sub>c0</sub>* led to a greater *C<sub>b,c</sub>*. In contrast, increasing *C<sub>b0</sub>* while maintaining constant *C<sub>c0</sub>* resulted in lower retention of suspended *P. putida*, suggesting that *P. putida* cells deposited onto attached kaolinite provided a less favorable collector surface.

[47] In conclusion, the experimental results presented herein suggest that the presence of kaolinite significantly inhibited the transport of *P. putida* in water-saturated columns packed with glass beads because *P. putida* could be attached onto kaolinite particles, which in turn could be retained by the solid matrix. The attachment of *P. putida* onto kaolinite was represented by a Langmuir-type isotherm. For both *P. putida* and kaolinite, the attachment and detachment rate coefficients increased with increasing flow rate, but the ratio of attachment to detachment rate coefficients decreased with increasing flow rate. The mathematical models presented satisfactorily simulated the *P. putida* and kaolinite data for all the transport and cotransport experiments.

**Notation**

- C<sub>b,eq</sub>* liquid phase concentration of bacteria at equilibrium, (*M* bacteria)/*L*<sup>3</sup>.
- C<sub>bc</sub>* concentration of bacteria attached onto suspended clay particles, (*M* bacteria)/(*M* clay).

$C_{bc}^*$	concentration of bacteria attached onto clay particles already attached onto glass beads, ( $M$ bacteria)/( $M$ clay).	$\Lambda_{b-b^*c^*}$	mass accumulation rate due to attachment of suspended bacteria onto clay particles already attached onto glass beads, ( $M$ bacteria)/( $L^3 t$ ).
$C_{bc_{eq}}$	concentration of bacteria attached onto suspended clay particles at equilibrium, ( $M$ bacteria)/( $M$ clay).	$\Lambda_{bc-b}$	mass accumulation rate due to bacteria detachment from suspended clay particles, ( $M$ bacteria)/( $L^3 t$ ).
$C_{bc_{eq}}^*$	concentration of bacteria attached onto clay particles already attached onto glass beads at equilibrium, ( $M$ bacteria)/( $M$ clay).	$\Lambda_{b^*c^*-b}$	mass accumulation rate due to detachment of bacteria from clay particles attached onto glass beads, ( $M$ bacteria)/( $L^3 t$ ).
$C_i$	concentration of species $i$ dissolved or suspended in the aqueous phase, $M/L^3$ .	$\Lambda_{bc-b^*c^*}$	mass accumulation rate due to attachment of suspended bacteria-clay particles onto glass beads, ( $M$ bacteria)/( $L^3 t$ ).
$C_i^*$	concentration of species $i$ attached onto the solid phase, ( $M$ of $i$ )/( $M$ solids).	$\Lambda_{b^*c^*-bc}$	mass accumulation rate due to detachment of attached bacteria-clay particles from glass beads, ( $M$ bacteria)/( $L^3 t$ ).
$C_{i_0}$	initial aqueous phase concentration of species $i$ , $M/L^3$ .	$\Phi_{tot}$	total intersurface potential energy (J), ( $M L^2$ )/ $t^2$ .
$C_{Total-b}$	total <i>P. putida</i> concentrations measured by plate counts on nutrient agar, ( $M$ bacteria)/ $L^3$ .		
$D_{e_i}$	effective diffusion coefficient of species $i$ , $L^2/t$ .		
$D_i$	hydrodynamic dispersion coefficient of species $i$ , $L^2/t$ .		
$i$	t (tracer), $b$ (bacteria), or $c$ (clay).		
$k_B$	Boltzmann's constant, ( $M L^2$ )/( $t^2 T$ ).		
$L$	column length, $L$ .		
$m_0$	zeroth absolute moment ( $M$ ).		
$M_n$	$n$ th normalized temporal moment, defined in (16).		
$M_r$	mass recovery, defined in (17).		
$n$	order of the moment.		
$Q^o$	maximum amount of bacteria that may be attached, ( $M$ bacteria)/( $M$ clay).		
$r_{i-i^*}$	attachment (deposition) rate coefficient of species $i$ onto glass beads, $1/t$ .		
$r_{i^*-i}$	detachment rate coefficient of species $i$ from glass beads, $1/t$ .		
$r_{b-bc}$	attachment rate coefficient of suspended bacteria onto suspended clay particles, ( $M$ clay)/( $M$ bacteria $t$ ).		
$r_{b-b^*c^*}$	attachment rate coefficient of suspended bacteria onto clay particles already attached onto glass beads, ( $M$ clay)/( $M$ bacteria $t$ ).		
$r_{bc-b}$	rate coefficient for bacteria detachment from suspended clay particles, $1/t$ .		
$r_{b^*c^*-b}$	rate coefficient of bacteria detachment from clay particles attached onto glass beads, $1/t$ .		
$r_{bc-b^*c^*}$	attachment rate coefficient of suspended bacteria-clay particles onto glass beads, $1/t$ .		
$r_{b^*c^*-bc}$	detachment rate coefficient of bacteria-clay particles from glass beads, $1/t$ .		
$t$	time, $t$ .		
$t_p$	injection time period, $t$ .		
$T$	temperature (K), $T$ .		
$U$	interstitial velocity, $L/t$ .		
$x$	Cartesian coordinate, $L$ .		
$\alpha_L$	longitudinal dispersivity, $L$ .		
$\alpha_1$	constant related to the attachment energy, $L^3$ /( $M$ bacteria).		
$\theta$	porosity of the column material, ( $L^3$ voids)/( $L^3$ solid matrix).		
$\rho_m$	bulk density of the solid matrix, $M/L^3$ .		
$\Lambda_{b-bc}$	mass accumulation rate due to attachment of suspended bacteria onto suspended clay particles, ( $M$ bacteria)/( $L^3 t$ ).		

[48] **Acknowledgments.** The authors are thankful to M. Kornaros, Chemical Engineering Department, University of Patras, for providing the *P. putida* microorganisms.

## References

- Abdel-Salam, A., and C. V. Chrysikopoulos (1995a), Analysis of a model for contaminant transport in fractured media in the presence of colloids, *J. Hydrol.*, *165*, 261–281.
- Abdel-Salam, A., and C. V. Chrysikopoulos (1995b), Modeling of colloid and colloid-facilitated contaminant transport in a two-dimensional fracture with spatially variable aperture, *Transp. Porous Media*, *20*(3), 197–221.
- Akbour, R. A., J. Douch, M. Hamdani, and P. Schmitz (2002), Transport of kaolinite colloids through quartz sand: Influence of humic acid,  $Ca^{2+}$ , and trace metals, *J. Colloid Interface Sci.*, *253*, 1–8.
- Anders, R., and C. V. Chrysikopoulos (2005), Virus fate and transport during artificial recharge with recycled water, *Water Resour. Res.*, *41*, W10415, doi:10.1029/2004WR003419.
- Artinger, R., T. Rabung, J. I. Kim, S. Sachs, K. Schmeide, K. H. Heise, G. Bernhard, and H. Nitsche (2002), Humic colloid-borne migration of uranium in sand columns, *J. Contam. Hydrol.*, *58*, 1–12.
- Auset, M., A. A. Keller, F. Brissaud, and V. Lazarova (2005), Intermittent filtration of bacteria and colloids in porous media, *Water Resour. Res.*, *41*, W09408, doi:10.1029/2004WR003611.
- Barton, C. D., and A. D. Karathanasis (2003), Influence of soil colloids on the migration of atrazine and zinc through large soil monoliths, *Water Air Soil Pollut.*, *14*, 3–21.
- Bear, J. (1979), *Hydraulics of Groundwater*, McGraw-Hill, New York.
- Becker, M. W., S. A. Collins, D. W. Metge, R. W. Harvey, and A. M. Shapiro (2004), Effect of cell physicochemical characteristics and motility on bacterial transport in groundwater, *J. Contam. Hydrol.*, *69*, 195–213.
- Bekhit, H. M., and A. E. Hassan (2007), Subsurface contaminant transport in the presence of colloids: Effect of nonlinear and nonequilibrium interactions, *Water Resour. Res.*, *43*, W08409, doi:10.1029/2006WR005418.
- Bekhit, H. M., M. A. El-Kordy, and A. E. Hassan (2009), Contaminant transport in groundwater in the presence of colloids and bacteria: Model development and verification, *J. Contam. Hydrol.*, *108*, 152–167.
- Bolster, C. H., B. Z. Haznedaroglu, and S. L. Walker (2009), Diversity in cell properties and transport behavior among 12 different environmental *Escherichia coli* isolates, *J. Environ. Qual.*, *38*, 465–472.
- Bradford, S. A., M. Bettahar, J. Simunek, and M. T. Genuchten (2004), Straining and attachment of colloids in physically heterogeneous porous media, *Vadose Zone J.*, *3*, 384–394.
- Camesano, T., and B. Logan (1998), Influence of fluid velocity and cell concentration on the transport of motile and nonmotile bacteria in porous media, *Environ. Sci. Technol.*, *32*, 1699–1708.
- Camesano, T., K. M. Unice, and B. Logan (1999), Blocking and ripening of colloids in porous media and their implications for bacterial transport, *Colloids Surf. A*, *160*, 291–308.
- Camper, A. K., J. T. Hayes, P. J. Sturman, W. L. Jones, and A. B. Cunningham (1993), Effects of motility and adsorption rate coefficient on

- transport of bacteria through saturated porous media, *Appl. Environ. Microbiol.*, *59*, 3455–3462.
- Choi, N. H., D. J. Kim, and S. B. Kim (2007), Quantification of bacterial mass recovery as a function of pore-water velocity and ionic strength, *Res. Microbiol.*, *158*, 70–78.
- Chrysikopoulos, C. V., and A. Abdel-Salam (1997), Modeling colloid transport and deposition in saturated fractures, *Colloids Surf. A*, *121*, 189–202.
- Chrysikopoulos, C. V., and Y. Sim (1996), One-dimensional virus transport homogeneous porous media with time dependent distribution coefficient, *J. Hydrol.*, *185*, 199–219.
- Chrysikopoulos, C. V., C. Masciopinto, R. La Mantia, and I. D. Manariotis (2010), Removal of biocolloids suspended in reclaimed wastewater by injection in a fractured aquifer model, *Environ. Sci. Technol.*, *44*(3), 971–977.
- Compere, F., G. Porel, and F. Delay (2001), Transport and retention of clay particles in saturated porous media: Influence of ionic strength and pore velocity, *J. Contam. Hydrol.*, *49*, 1–21.
- Corapcioglu, M. Y., and S. Kim (1995), Modeling facilitated contaminant transport by mobile bacteria, *Water Resour. Res.*, *31*, 2639–2647.
- Dabros, T., and T. G. M. van de Ven (1982), Kinetics of coating by colloid particles, *J. Colloid Interface Sci.*, *89*, 232–244.
- de Jonge, L. W., P. Moldrup, G. H. Rubæk, K. Schelde, and J. Djurhuus (2004), Particle leaching and particle-facilitated transport of phosphorus at the field scale, *Vadose Zone J.*, *3*, 462–470.
- Dong, H., T. D. Scheibe, W. P. Johnson, C. M. Monkman, and M. E. Fuller (2006), Change of collision efficiency with distance in bacterial transport experiments, *Ground Water*, *44*, 415–429.
- Fontes, D. E., A. L. Mills, G. M. Hornberger, and J. S. Herman (1991), Physical and chemical factors influencing transport of microorganisms through porous media, *Appl. Environ. Microbiol.*, *57*, 2473–2481.
- Foppen, J. W. A., and J. F. Schijven (2005), Transport of *E. coli* in columns of geochemically heterogeneous sediment, *Water Res.*, *39*, 3082–3088.
- Gannon, J. T., V. B. Maniail, and M. Alexander (1991), Relationships between cell surface properties and transport of bacteria through soil, *Appl. Environ. Microbiol.*, *57*, 190–193.
- Gear, C. W. (1971), The automatic integration of ordinary differential equations, *Commun. ACM*, *14*, 176–179.
- Harter, T., S. Wagner, and E. R. Atwill (2000), Colloid transport and filtration of *Cryptosporidium parvum* in sandy soils and aquifer sediments, *Environ. Sci. Technol.*, *34*, 62–70.
- Hendry, M. J., J. R. Lawrence, and P. Maloszewski (1999), Effect of velocity on the transport of two bacteria through saturated sand, *Ground Water*, *37*, 103–112.
- Ho, Y. S., J. C. Y. Ng, and G. McKay (2001), Removal of lead(II) from effluents by sorption on peat using second-order kinetics, *Sep. Sci. Technol.*, *36*, 241–261.
- James, S. C., and C. V. Chrysikopoulos (1999), Transport of polydisperse colloid suspensions in a single fracture, *Water Resour. Res.*, *35*(3), 707–718.
- James, S. C., and C. V. Chrysikopoulos (2003), Effective velocity and effective dispersion coefficient for finite-sized particles flowing in a uniform fracture, *J. Colloid Interface Sci.*, *263*, 288–295.
- James, S. C., T. K. Bilezikjian, and C. V. Chrysikopoulos (2005), Contaminant transport in a fracture with spatially variable aperture in the presence of monodisperse and polydisperse colloids, *Stochastic Environ. Res. Risk Assess.*, *19*(4), 266–279, doi:10.1007/s00477-004-0231-3.
- Jewett, D. G., T. A. Hilbert, B. E. Logan, R. G. Arnold, and R. C. Bales (1995), Bacterial transport in laboratory columns and filters: Influence of ionic strength and pH on collision efficiency, *Water Res.*, *29*, 1673–1680.
- Jiang, D., Q. Huang, P. Cai, X. Rong, and W. Chen (2007), Adsorption of *Pseudomonas putida* on clay minerals and iron oxide, *Colloids Surf. B*, *54*, 217–221.
- Keller, A. A., S. Sirivithayapakorn, and C. V. Chrysikopoulos (2004), Early breakthrough of colloids and bacteriophage MS2 in a water-saturated sand column, *Water Resour. Res.*, *40*, W08304, doi:10.1029/2003WR002676.
- Kersting, A. B., D. W. Efurud, D. L. Finnegan, D. J. Rokop, D. K. Smith, and J. L. Thompson (1999), Migration of plutonium in groundwater at the Nevada test site, *Nature*, *397*, 56–59.
- Kim, S. B., S. J. Park, C. G. Lee, N. C. Choi, and D. J. Kim (2008), Bacteria transport through goethite-coated sand: Effects of solution pH and coated sand content, *Colloids Surf. B*, *63*, 236–242.
- Kretzschmar, R., and H. Sticher (1997), Transport of humic-coated iron oxide colloids in a sandy soil: Influence of  $\text{Ca}^{2+}$  and trace metals, *Environ. Sci. Technol.*, *31*, 3497–3504.
- Leon-Morales, C. F., A. P. Leis, M. Strathmann, and H. C. Flemming (2004), Interactions between laponite and microbial biofilms in porous media: Implications for colloid transport and biofilm stability, *Water Res.*, *38*, 3614–3626.
- Lindqvist, R., and C. G. Enfield (1992), Biosorption of dichlorodiphenyltrichloroethane and hexachlorobenzene in groundwater and its implications for facilitated transport, *Appl. Environ. Microbiol.*, *58*, 2211–2218.
- Liu, D., P. R. Johnson, and M. Elimelech (1995), Colloid deposition dynamics in flow through porous media: Role of electrolyte concentration, *Environ. Sci. Technol.*, *29*, 2963–2973.
- Liu, Z., and K. Papadopoulos (1995), Chemotaxis in near-linear gradients of chemoattractants, *Appl. Environ. Microbiol.*, *61*, 3567–3572.
- Masciopinto, C., R. La Mantia, and C. V. Chrysikopoulos (2008), Fate and transport of pathogens in a fractured aquifer in the Salento area, Italy, *Water Resour. Res.*, *44*, W01404, doi:10.1029/2006WR005643.
- Maxwell, R. M., C. Welty, and R. W. Harvey (2007), Revisiting the Cape Cod bacteria injection experiment using a stochastic modeling approach, *Environ. Sci. Technol.*, *41*, 5548–5558.
- Mibus, J., S. Sachs, W. Pflingsten, C. Nebelung, and G. Bernhard (2007), Migration of uranium(IV)/(VI) in the presence of humic acids in quartz sand: A laboratory column study, *J. Contam. Hydrol.*, *89*, 199–217.
- Newman, M. E., A. W. Elzerman, and B. B. Looney (1993), Facilitated transport of selected metals in aquifer material packed columns, *J. Contam. Hydrol.*, *14*, 233–246.
- Ouyang, Y., D. Shinde, R. S. Mansell, and W. Harris (1996), Colloid-enhanced transport of chemicals in subsurface environments: A review, *Crit. Rev. Environ. Sci. Technol.*, *26*, 189.
- Pang, L., and J. Simunek (2006), Evaluation of bacteria-facilitated cadmium transport in gravel columns using HYDRUS colloid-facilitated solute transport model, *Water Resour. Res.*, *42*, W12S10, doi:10.1029/2006WR004896.
- Pang, L., M. Noonan, M. Flintoft, and P. van den Brink (2005), A laboratory study of bacteria-facilitated cadmium transport in alluvial gravel aquifer media, *J. Environ. Qual.*, *34*, 237–247.
- Petzold, L. R. (1983), *A description of DASSL A differential/algebraic system solver*, in *Scientific Computing*, edited by R. S. Stepleman, pp. 65–1, North Holland, Amsterdam.
- Powelson, D. K., and A. L. Mills (2001), Transport of *Escherichia coli* in sand columns with constant and changing water contents, *J. Environ. Qual.*, *30*, 238–245.
- Redman, J. A., S. L. Walker, and M. Elimelech (2004), Bacterial adhesion and transport in porous media: Role of the secondary energy minimum, *Environ. Sci. Technol.*, *38*, 1777–1785.
- Rickwood, D., T. Ford, and J. Graham (1982), Nycodenz: A new nonionic iodinated gradient medium, *Anal. Biochem.*, *123*, 23–31.
- Rijnaarts, H. H. M., W. Norde, E. J. Bouwer, J. Lyklema, and A. J. B. Zehnder (1996), Bacterial deposition in porous media related to the clean bed collision efficiency and to substratum blocking by attached cells, *Environ. Sci. Technol.*, *30*, 2869–2876.
- Rong, X., Q. Huang, X. He, H. Chen, P. Cai, and W. Liang (2008), Interaction of *Pseudomonas putida* with kaolinite and montmorillonite: A combination study by equilibrium adsorption, ITC, SEM and FTIR, *Colloids Surf. B*, *64*, 49–55.
- Rong, X., W. Chen, Q. Huang, P. Cai, and W. Liang (2010), *Pseudomonas putida* adhesion to goethite: Studied by equilibrium adsorption, SEM, FTIR and ITC, *Colloids Surf. B*, *80*, 79–85.
- Saiers, J. E., and G. M. Hornberger (1996), The role of colloidal kaolinite in the transport of cesium through laboratory sand columns, *Water Resour. Res.*, *32*(1), 33–41.
- Severino, G., V. Cvetkovic, and A. Coppola (2007), Spatial moments for colloid-enhanced radionuclide transport in heterogeneous aquifers, *Adv. Water Res.*, *30*, 101–112.
- Shiratori, K., Y. Yamashita, and Y. Adachi (2007), Deposition and subsequent release of Na-kaolinite particles by adjusting pH in the column packed with Toyoura sand, *Colloids Surf. A*, *306*, 137–141.
- Sim, Y., and C. V. Chrysikopoulos (1995), Analytical models for one-dimensional virus transport in saturated porous media, *Water Resour. Res.*, *31*(5), 1429–1437. (Correction, *Water Resour. Res.*, *32*(5), 1473, 1996.)
- Simoni, S. F., H. Harms, T. N. P. Bosma, and A. J. B. Zehnder (1998), Population heterogeneity affects transport of bacteria through sand columns at low flow rates, *Environ. Sci. Technol.*, *32*, 2100–2105.
- Smith, J., B. Gao, H. Funabashi, T. N. Tran, D. Luo, B. A. Ahner, T. S. Steenhuis, A. G. Hay, and M. T. Walter (2008), Pore-scale quantification of colloid transport in saturated porous media, *Environ. Sci. Technol.*, *42*, 517–523.

- Stephan, E. A., and G. G. Chase (2001), A preliminary examination of zeta potential and deep bed filtration activity, *Sep. Purif. Technol.*, *21*, 219–226.
- Stevik, T. K., K. Aa, G. Ausland, and J. F. Hanssen (2004), Retention and removal of pathogenic bacteria in wastewater percolating through porous media: A review, *Water Res.*, *38*, 1355–1367.
- Syngouna, V. I., and C. V. Chrysikopoulos (2010), Interaction between viruses and clays in static and dynamic batch systems, *Environ. Sci. Technol.*, *44*, 4539–4544.
- Tan, Y., J. T. Gannon, P. Baveye, and M. Alexander (1994), Transport of bacteria in aquifer sand: Experiments and model simulations, *Water Resour. Res.*, *30*, 3243–3252.
- Tatalovich, M. E., K. Y. Lee, and C. V. Chrysikopoulos (2000), Modeling the transport of contaminants originating from the dissolution of DNAPL pools in aquifers in the presence of dissolved humic substances, *Transp. Porous Media*, *38*(1/2), 93–115.
- Tien, N. C., and C. P. Jen (2007), Analytical modeling for colloid-facilitated transport of N-member radionuclides chains in the fractured rock, *Nucl. Sci. Tech.*, *18*(6), 336–343.
- Tong, M., X. Li., C. N. Brow, and W. P. Johnson (2005), Detachment-influenced transport of an adhesion-deficient bacterial strain within water-reactive porous media, *Environ. Sci. Technol.*, *39*, 2500–2508.
- Upadhyayula, V. K. K., S. Deng, G. B. Smith, and M. C. Mitchell (2009), Adsorption of *Bacillus subtilis* on single-walled carbon nanotube aggregates, activated carbon and NanoCeram, *Water Res.*, *43*, 148–156.
- Villholth, K. G., N. J. Jarvis, O. H. Jacobsen, and H. de Jonge (2000), Field investigations and modeling of particle-facilitated pesticide transport in microporous soil, *J. Environ. Qual.*, *29*, 1298–1309.
- Yates, M. V., C. P. Gerba, and L. M. Kelly (1985), Virus persistence in groundwater, *Appl. Environ. Microbiol.*, *49*, 778–781.
- Walshe, G. E., L. Pang, M. Flury, M. E. Close, and M. Flintoft (2010), Effects of pH, ionic strength, dissolved organic matter, and flow rate on the co-transport of MS2 bacteriophages with kaolinite in gravel aquifer media, *Water Res.*, *44*, 1255–1269.

---

C. V. Chrysikopoulos and I. A. Vasiliadou, Environmental Engineering Laboratory, Civil Engineering Department, University of Patras, GR-26500 Patras, Greece. (gios@upatras.gr; ivasiliadou@upatras.gr)